Available online at www.sciencedirect.com

ScienceDirect

Microelectronic Engineering 86 (2009) 249–258

MICROELECTRONIC ENGINEERING

www.elsevier.com/locate/mee

Density functional theory study of first-layer adsorption of ZrO_2 and HfO_2 on Ge(1 0 0)

T.J. Grassman, S.R. Bishop, A.C. Kummel *

University of California, San Diego, Department of Chemistry/Biochemistry, 9500 Gilman Drive #0358, La Jolla, CA 92093-0358, United States

Received 26 September 2007; accepted 27 December 2007
Available online 12 February 2008

Abstract

Density functional theory was used to performed a survey of transition metal oxide ($MO_2 = ZrO_2$, HfO_2) ordered molecular adsorbate bonding configurations on the Ge(1 0 0)-4 × 2 surface. Surface binding geometries of metal-down (O–M–Ge) and oxygen-down (M–O–Ge) were considered, including both adsorbate and displacement geometries of M–O–Ge. Calculated enthalpies of adsorption show that bonding geometries with metal–Ge bonds (O–M–Ge) are essentially degenerate with oxygen–Ge bonding (M–O–Ge). Calculated electronic structures indicate that adsorbate surface bonding geometries of the form O–M–Ge tend to create a metallic interfaces, while M–O–Ge geometries produce, in general, much more favorable electronic structures. Hydrogen passivation of both oxygen and metal dangling bonds was found to improve the electronic structure of both types of MO_2 adsorbate systems, and induced the opening of true semiconducting band gaps for the adsorbate-type M–O–Ge geometries. Shifts observed in the DOS minima for both O–M–Ge and M–O–Ge adsorbate geometries are consistent with surface band bending induced by the adsorbate films, where such band bending extends much further into the Ge substrate than can be modeled by the Ge slabs used in this work.

Keywords: Ge; Germanium; MOSFET; High-*k* dielectric; Zirconium oxide; Hafnium oxide; Semiconductor-oxide interface

1. Introduction

Due to the approach of the fundamental limits of classical silicon CMOS scaling, recent years have seen a great deal of work focused on alternative channel materials for high-speed MOS-type field-effect transistors. One such alternative material is germanium, whose greater low-field intrinsic carrier mobilities may provide for a significant increase in saturation current over state-of-the-art silicon MOSFET devices. However, in contrast to Si, Ge does not have a suitably stable electrically-passivating native oxide. The Ge native oxide, GeO_2, is both water-soluble and thermally unstable at elevated temperatures; GeO_2 decomposes and desorbs as GeO above 400 °C [1–3]. Therefore, an alternative dielectric and/or electrical passivation method is needed.

Numerous experiments have attempted the fabrication of Ge-based MOSFET or MOSCAP devices using a great diversity of insulators, including GeO_2 [4–6], Ge_3N_4 [7], GeO_xN_y [5,8,9], SiO_2 (with and without a Si interlayer/cap) [10,11], and high-*k* metal oxides ($BaStTiO_3$, ZrO_2, HfO_2) [12–14]. The success of these different dielectric materials has been found to depend greatly on the nature of the semiconductor-oxide interface. The most studied, and probably most successful, gate dielectric materials are the transition metal dioxides ZrO_2 and HfO_2 (denoted as MO_2 in this manuscript), usually grown by atomic layer deposition (ALD). These oxides, under normal Ge processing conditions, are amorphous, and depending on initial native oxide content (as well as composition) on the Ge(1 0 0) surface, the oxide/Ge interface may be either abrupt or contain some germanate interlayer (though these interlayers are thinner than those found with Si). High resolution TEM imaging indicates that ZrO_2 tends to form more abrupt interfaces, while HfO_2 has been shown to be

---

* Corresponding author. Tel.: +1 858 534 3368; fax: +1 858 534 2063.
E-mail address: akummel@ucsd.edu (A.C. Kummel).

0167-9317/$ - see front matter © 2008 Elsevier B.V. All rights reserved.
doi:10.1016/j.mee.2007.12.087

more likely to form interfacial interlayers [15]. The TEM images also seem to indicate that the abrupt oxide/Ge interface may be somewhat ordered, even though the rest of the oxide layer is amorphous.

MOSFET (and MOSCap) device quality is found to vary greatly in these MO_2/Ge(100) gate stacks, with the trend closely related to the oxide-semiconductor interface quality and composition (i.e. clean vs. oxidized surface, native oxide vs. oxynitride, abrupt vs. interlayer interface, etc.) [16]. Currently available data, however, is not accurate or precise enough to sufficiently characterize the oxide/Ge interface, so detailed conclusions about the exact causes of problems related to the interface in these devices are unable to be made. It is hoped that carefully performed high resolution scanning transmission electron microscopy (STEM) will enable a close look at the structure at the oxide/semiconductor interface to reveal the extent of order at these interfaces and to elucidate the basic bonding structure as metal–O–Ge, O–metal–Ge, or a combination of the two.

We have performed a survey of potential ordered oxide/semiconductor interface structures between stoichiometric molecular ZrO_2/HfO_2 and Ge(100), considering both surface coverage and surface binding configuration (O–metal–Ge bonding vs. metal–O–Ge bonding) using density functional theory (DFT) modeling. This work is by no means intended to be an exhaustive set of structures, but merely an attempt to provide some insight into the MO_2/Ge interfacial system. Additionally, these structures will serve as precursors to later computational studies of thick amorphous MO_2 layers on Ge(100).

2. Methods

All density functional theory (DFT) calculations presented in this paper were performed using the Vienna Ab-Initio Simulation Package (VASP) [17–20] in the generalized gradient approximation (PBE exchange-correlation functional), with projector augmented wave (PAW) potentials [21,22] (as supplied by the VASP group), a 4 × 4 × 1 Monkhorst-Pack *k*-point mesh generation scheme (for a total of four irreducible *k*-points), and plane-wave basis cut-off of 450 eV. All parameters (i.e. *k*-points, cut-off energy, vacuum space, slab thickness, etc.) were chosen such that they were each individually converged to within 1 meV/atom for the system of study. The absolute error of this type of calculation is estimated to be up to 0.37 eV [23], but it is difficult to estimate the exact error with respect to the SiO/Ge(100) system presented in this report. Regardless of absolute numerical accuracy, the qualitative results from these calculations should be quite reasonable because comparisons are being made merely between different bonding geometries that have all been calculated under identical conditions and with similar types of bonds. Therefore, the calculations in this paper should have good relative accuracy, with an estimated relative error of ±0.1 eV [24].

The system studied consisted of an Ge(100) slab supercell with a 4 × 2 surface dimer reconstruction, as this is the lowest energy configuration (compared to the 2 × 1 flat dimer and 1 × 1 unreconstructed geometries). The germanium slab was eight atomic layers thick, with each layer being 2 × 4 atoms in area, for a total of 64 Ge atoms per unit cell (for the clean, Ge surface/substrate calculations), shown in Fig. 1a (inlay). The bottom of the slab was unreconstructed and terminated with 16 hydrogen atoms (two H atoms per Ge). The clean Ge supercell contained 12 atomic layers of vacuum space in the *z*-direction. The bottom three Ge layers were constrained to the minimum-energy bulk DFT geometry, which was found through a series of bulk Ge calculations to have a lattice parameter of 5.795 Å (2.4% larger than the experimental result of 5.658 Å due to the well-known GGA overestimation of lattice parameters). The terminating H atoms were initially allowed to relax and were kept fixed at these optimized positions for all subsequent calculations. All other atoms (upper substrate, adsorbate, gas-phase) were allowed to

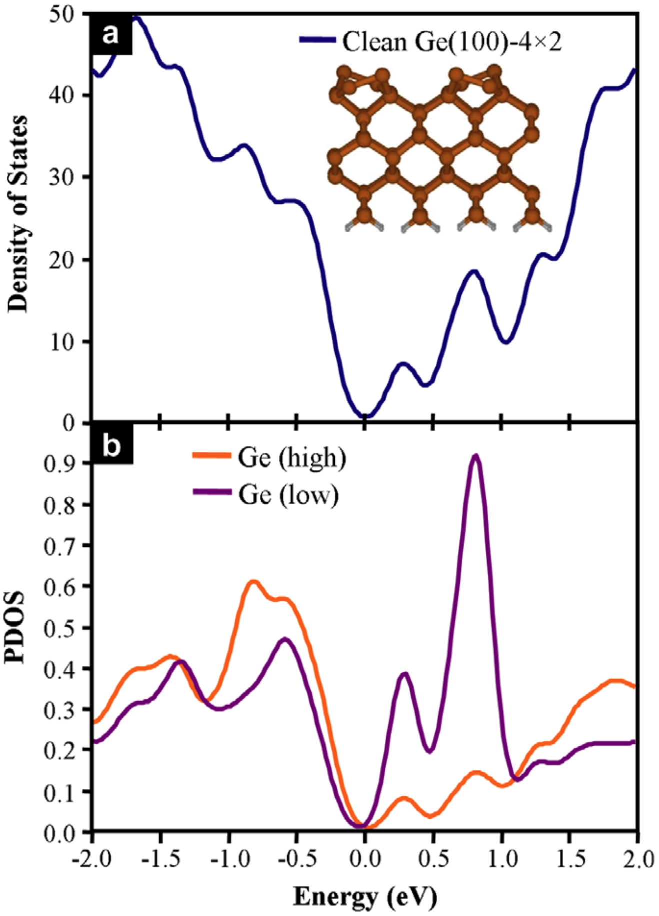

Fig. 1. DFT calculated (a) density of states, DOS, and (b) projected densities of states, PDOS, for clean Ge(100)-4 × 2. Note the different electronic structures for the high vs. low Ge surface dimer atoms, where the sp^2-like low atom has a large empty-state (CB) density, while the sp^3-like high atom has a greater filled-state (VB) density.

structurally relax with respect to interatomic forces to a tolerance of 0.01 eV/Å.

3. Results and discussion

Metal oxide molecules ($MO_2 = ZrO_2$, HfO_2) were placed on the Ge(1 0 0)-4 × 2 surface at appropriate (chemically sensible) coverages in two different surface binding configurations: O–M–Ge, where the metal atoms bond directly to the Ge surface, and M–O–Ge, where the oxygen atoms bond directly to the Ge surface. The M–O–Ge configuration also consisted of two distinct sub-configurations: displacement-type, where the O atoms displace surface Ge atoms, and adsorbate-type, where the O atoms bind to the dangling bonds of the Ge atoms. Adsorption enthalpies were extracted from these calculations using the Hess's law method of "products minus reactants." A summary of the geometries modeled and their calculated enthalpies of adsorption can be found in Table 1. The systems were also analyzed for electronic structure (density of states) information in order to determine passive or pinning oxide bonding to the surface.

It must be noted, however, that there are well-known problems with standard LDA- and GGA-based DFT with respect to the electronic structures of semiconducting and insulating materials, namely a general underestimation of the band gap by 30–100%, due to the approximation of the exchange potential [25,26]. Unfortunately, this problem is at its worst for small band gap semiconductors, such as germanium. In fact, standard DFT predicts a slight overlap of the Ge VB maximum and CB minimum, producing a semi-metallic electronic structure (see Fig. 1a). Clearly these calculations would benefit from being performed under a higher-level of theory, such as the inclusion of exact exchange (i.e. hybrid functionals). We do intend to perform this work, but as these higher-level calculations are about two orders of magnitude more expensive that standard DFT, they are far from being completed.

However, because there is still a significant minimum in the DOS at the Fermi level, it is possible to extract useful information from standard DFT calculations of Ge(1 0 0). Specifically, one may compare the calculated DOS of the clean Ge(1 0 0)-4 × 2 slab with the DOS of the various

Table 1

Summary of computational results for ordered molecular adsorption of MO_2 on the Ge(1 0 0) surface, including ball-and-stick diagram and calculated enthalpies of adsorption

Identification	Geometry	Δh_{ads} (ZrO_2)[a] (eV)	Δh_{ads} (HfO_2)[a] (eV)
Half-coverage O–M–Ge adsorption	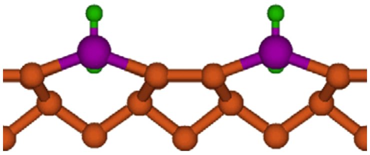	−3.16	−3.63
Full-coverage O–M–Ge adsorption	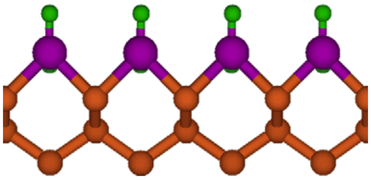	−2.78	−3.29
Half-coverage M–O–Ge displacement	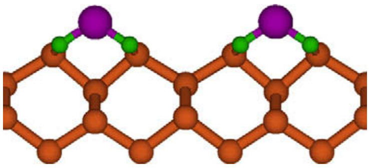	−1.62	−2.13
Half-coverage M–O–Ge adsorption	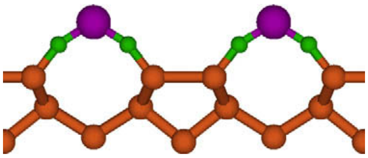	−2.97	−3.67

[a] Calculated adsorption energies, Δh_{ads}, are given with respect to the clean Ge(1 0 0)-4 × 2 surface and single SiO molecules. Displacement sites are calculated with respect to the creation of Ge ad-dimers.

Ge(1 0 0) slabs with oxygen adsorbates on them. Because we are particularly interested in the induction of electronic states within the band gap, a potential cause of Fermi level pinning, special attention will be paid to the near-Fermi level region of the calculated densities of states. There are two general possible conditions related to the DOS after the addition of the metal oxide adsorbates to the Ge(1 0 0) surface: (a) the DOS at the near-E_F region decreases (or exhibits no change) after the addition of the MO_2 adsorbates, or (b) the DOS at the near-E_F region increases after the addition of the MO_2 adsorbates. If the DOS decreases or shows no change, it is reasonable to conclude that the adsorbate is not a potential source of Fermi level pinning, while if the DOS increases it is reasonable to conclude that pinning is possible because of the induction of band gap or band edge states that are consistent with Fermi level pinning.

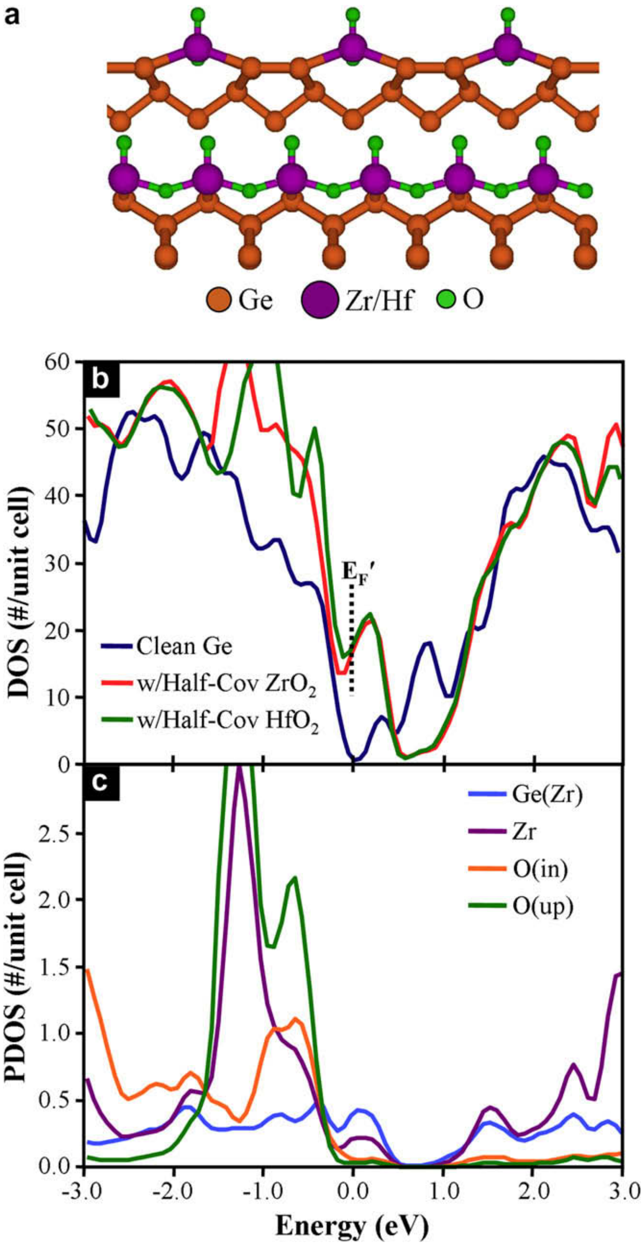

Fig. 2. (a) Ball-and-stick diagrams of the half-coverage O–M–Ge geometry. (b) DFT calculated densities of states for half-coverage O–M–Ge ZrO_2 and HfO_2. (c) Projected density of states for ZrO_2 case (note: HfO_2 results nearly identical).

For the sake of comparison between the clean Ge(1 0 0)-4 × 2 and MO_2 adsorbate-covered Ge(1 0 0) surfaces, we align the calculated densities of states using the Ge band edge located at about −12 eV (the deepest Ge-based DOS feature available in these calculations). Because of the lack of band gap in these simulations the calculated Fermi level for the majority of the various systems modeled has little meaning. Therefore, the calculated Fermi level for the MO_2/Ge(1 0 0) systems shall be indicated in the DOS figures but shall not be considered in the analysis of most of the computational results. In the case where the calculated Fermi level of a MO_2/Ge(1 0 0) system actually is meaningful (e.g. in the case where the MO_2 adsorption yields a system band gap), it shall be pointed out and discussed. The x-axis (energy) on each presented DOS figure in this manuscript is reliable only for the clean Ge(1 0 0)-4 × 2 plot.

With this method of DOS alignment, we can directly visualize any changes in the density of states that may have occurred due to the addition of MO_2 molecules, particularly any changes at or near the clean Ge(1 0 0) near-E_F (i.e. the zero volts position). The projected density of states (PDOS), which is essentially the local DOS for each individual atom in the computational system (e.g. see Fig. 1b for PDOS of the two different Ge surface dimer atoms), can provide additional insight into any observed changes in the electronic structure.

3.1. O–M–Ge surface binding of MO_2 on Ge(1 0 0)

3.1.1. Half-coverage O–M–Ge adsorption

To simulate a metal–Ge interface at the first-layer of MO_2 on the Ge(1 0 0) surface molecular ZrO_2 and HfO_2 were adsorbed to the surface in a metal-down, or O–M–Ge, bonding configuration (see Fig. 2a). Such a configuration models atomic layer deposition (ALD) growth in which the metal atoms are deposited first onto the clean surface. In this particular O–M–Ge geometry, the metal atom binds directly to the Ge dangling bonds, with half the oxygen atoms pointing upward (away from the surface) and half sideways, bonding with the next metal atom over. This particular system only utilizes half of the number of available Ge bonding sites (i.e. in this case the Ge–Ge surface dimers are left intact), and is designated half-coverage. This geometry yielded enthalpies of adsorption for the MO_2/Ge(1 0 0) system of −3.16 eV/ZrO_2 and −3.63 eV/HfO_2.

The half-coverage O–M–Ge configuration was found to induce a large DOS at the zero-volt position (which is very close to the system's calculated Fermi level), as seen in the system densities of states from both ZrO_2 and HfO_2 cases, shown in Fig. 2b. The PDOS for the ZrO_2 case is presented in Fig. 2c (the PDOS for HfO_2 is nearly identical). The increased DOS appears to be a result of a downward shift of the near-E_F CB states belonging to the sp^2-like (i.e. mostly empty dangling bond) “low” buckled dimer atoms as they are forced flat by the bonding of the MO_2 adsorbates. On the clean Ge(100) surface, flat dimers possess exactly half-filled dangling bonds, which produces small metallic states within the band gap [27]. Therefore, it seems that the metal–Ge bonds being formed in this O–M–Ge adsorbate configuration may be more metallic in nature than covalent, where we would expect to see these states shifted out of the near-E_F region due to the molecular orbital split into sigma bonding and antibonding states.

3.1.2. Half-coverage H–O–M–Ge adsorption

The upward pointing oxygen atoms in the previous O–M–Ge adsorbate geometry have partially-filled dangling bonds and simple reasoning indicates that they may possess electronic states near or at the Fermi level, possibly playing a role in the large observed induction of near-E_F DOS. It is also possible, given the high electronegativity of oxygen atoms, that they could be withdrawing excessive amounts of charge from the Zr/Hf atoms, thereby inducing the observed DOS shift. Passivation of these dangling bonds with H atoms would eliminate the partially-filled dangling bonds and limit the O atoms’ capacity for charge withdrawal from the neighboring metal atoms. Additionally, the termination of the O dangling bonds would act in a similar manner as further oxide growth, comparable to the use of H passivation on the bottom of the Ge slab.

Fig. 3 presents the results of the H passivation of the half-coverage O–M–Ge adsorption geometry. We find that while the passivation has indeed eliminated much of the near-E_F oxygen DOS, it has not removed the increased DOS at the Fermi level (see Fig. 3b). In fact, the PDOS for the surface Ge and Zr atoms has actually slightly increased as a result, seen in Fig. 3c. Most likely this is actually a consequence of charge being forced back into the metal atoms (because of the charge withdrawal limitations placed upon the O atoms by the H passivation), and thereby back into the metallic M–Ge bonding states.

For both the passivated and unpassivated O–M–Ge geometries we consider the shift of the near-E_F DOS minima (see Figs. 2b and 3b), especially the gap-like situation seen for the H–O–M–Ge case. A possible explanation for this behavior is band bending induced by the MO_2 adsorbate films. For a thick doped sample, band bending should induce a decrease or elimination of an observable band gap in the total DOS. However, band bending for an intrinsic semiconductor is expected to extend much further into the semiconductor than can be modeled with the current Ge(100) slab. Therefore, for the eight layer intrinsic slab employed in our calculations, the band bending should appear as just a shift in the band gap (or DOS minimum) with respect to the original clean Ge(100)-4 × 2 DOS minimum, such as that observed for the O–M–Ge adsorbate geometries.

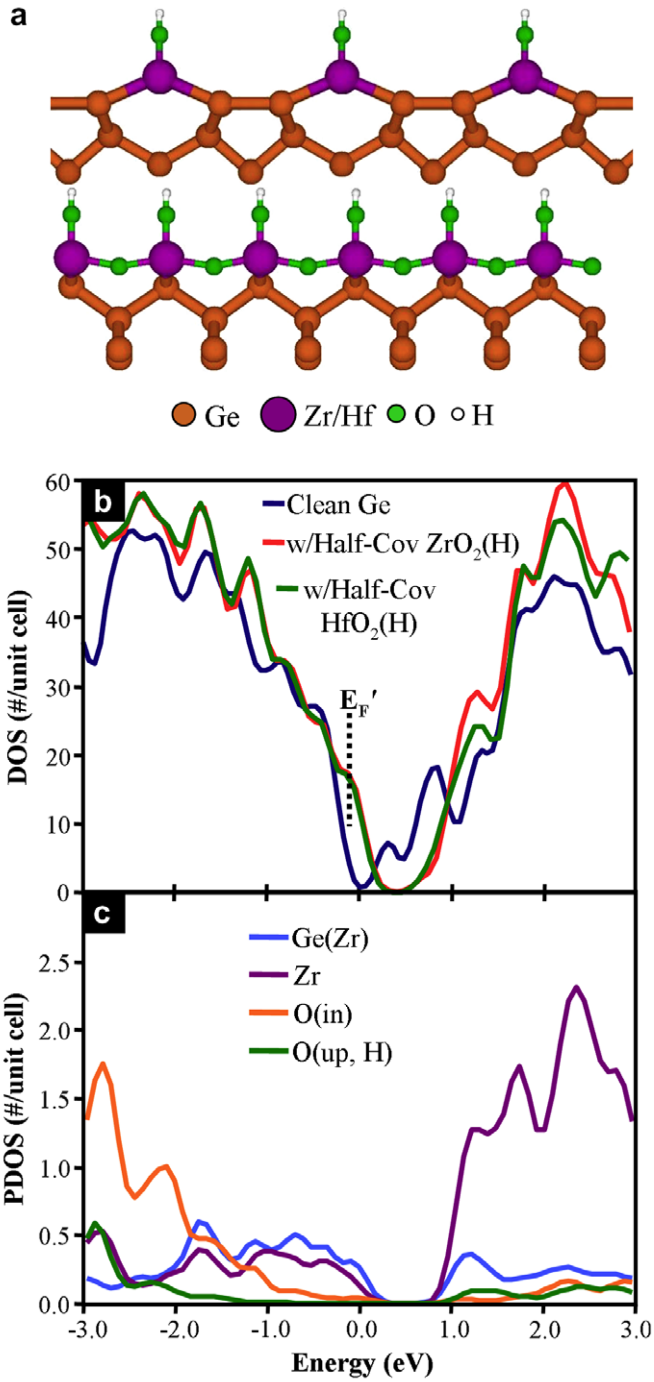

Fig. 3. (a) Ball-and-stick diagrams of the half-coverage H–O–M–Ge geometry. (b) DFT calculated densities of states for half-coverage H–O–M–Ge ZrO_2 and HfO_2. (c) Projected density of states for ZrO_2 case (note: HfO_2 results nearly identical). Note the shift in DOS minima for both species.

3.1.3. Full-coverage H–O–M–Ge adsorption

As a final check into the O–M–Ge type adsorbate bonding configuration, metal oxide molecules were also inserted into the Ge dimers, giving a full-coverage MO_2/Ge(100) system (see Fig. 4a). We present only the H-passivated version of this geometry because the difference between the passivated and the non-passivated geometries is the same as for the half-coverage case (the removal of some of the near-E_F oxygen DOS makes for easier visualization). This full-coverage geometry produces a network of –M–Ge–M– bonding, compared to the half-coverage case where the metal atoms were always separated by two Ge atoms (–M–Ge–Ge–M–). If the hypothesis of metallic M–Ge bonding derived from the half-coverage case is valid, we would expect the full-coverage case to display even greater metallic bonding character. The average adsorption energy per MO_2 molecule calculated for the full-coverage case was −2.78 eV/ZrO_2 and −3.29 eV/HfO_2, noticeably lower than for the half-coverage case but still considerably exothermic.

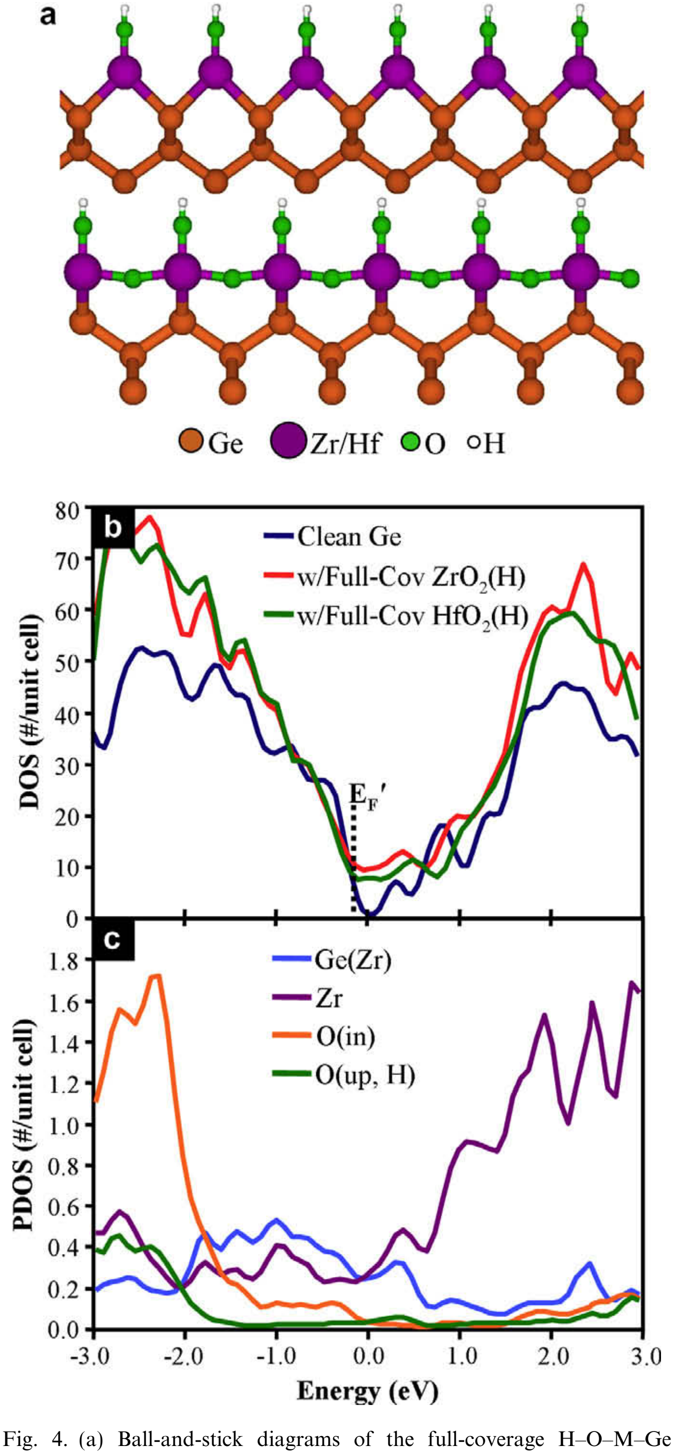

Fig. 4. (a) Ball-and-stick diagrams of the full-coverage H–O–M–Ge geometry. (b) DFT calculated densities of states for full-coverage H–O–M–Ge ZrO_2 and HfO_2. (c) Projected density of states for ZrO_2 case (note: HfO_2 results nearly identical).

As shown in Fig. 4b, the metallic DOS near and at the Fermi level is indeed greatly increased. The calculated PDOS, given in Fig. 4c, indicates the near-E_F DOS is primarily due to the surface Ge and metal atoms, just like in the half-coverage geometries, but in this case there is no minimum above the Fermi level. Since there is no shifted band gap, the issue of band bending is probably not relevant. Therefore, even within the limited accuracy of the DOS calculations, the greatly increased PDOS of the metal–Ge bonding network demonstrates a clear metallic nature, which is likely to cause problems in a MOSFET device.

3.2. *M–O–Ge surface binding of MO_2 on Ge(1 0 0)*

3.2.1. *Half-coverage M–O–Ge displacement*

To simulate an oxygen–Ge interface for the first-layer of MO_2 on the Ge(1 0 0), surface molecular ZrO_2 and HfO_2 were adsorbed to the surface in an oxygen-down, or M–O–Ge, bonding configuration via a Ge displacement reaction. Two M–O–Ge bonding geometries were studied: the first consists of oxygen displacement of surface Ge atoms (see Fig. 5a), similar to that seen in the case of the oxidation reaction of Ge(1 0 0), while the second M–O–Ge binding geometry is a simple adsorption bonding configuration. The displacement geometry replaces all of the surface Ge atoms with O atoms, and includes one metal atom for every two oxygen atoms to maintain the MO_2 stoichiometry. Because this system contains the same number of MO_2 molecules as the half-coverage O–M–Ge, it is also denoted as half-coverage. This geometry yielded enthalpies of adsorption for the MO_2/Ge(1 0 0) system of −1.62 eV/ZrO_2 and −2.13 eV/HfO_2 (note: these enthalpies include the formation enthalpy of Ge ad-dimers by the displaced Ge atoms). These enthalpies are considerably lower than for the O–M–Ge cases, as well as the other M–O–Ge that shall be discussed later in this report. With such comparatively low adsorption energies, we would not expect this site to form, and one might actually expect molecules of this sort of desorb from the surface at standard processing temperatures (500–600 °C).

Regardless of the low adsorption energy, it is insightful to examine the calculated electronic structures for the displacement-type M–O–Ge geometry. As seen in Fig. 5b, there is an increase in the near-E_F DOS for the MO_2/Ge(1 0 0) systems, but the minima are still located at basically the same spot as the clean Ge(1 0 0)-4 × 2 minimum. There is a noticeable decrease in filled-state density (VB) and an increase in empty-state density (CB); the calculated Fermi level is found to reside 0.3 eV above the clean Ge(1 0 0) position due to the different filling of electronic states resulting from the change in DOS. The PDOS for

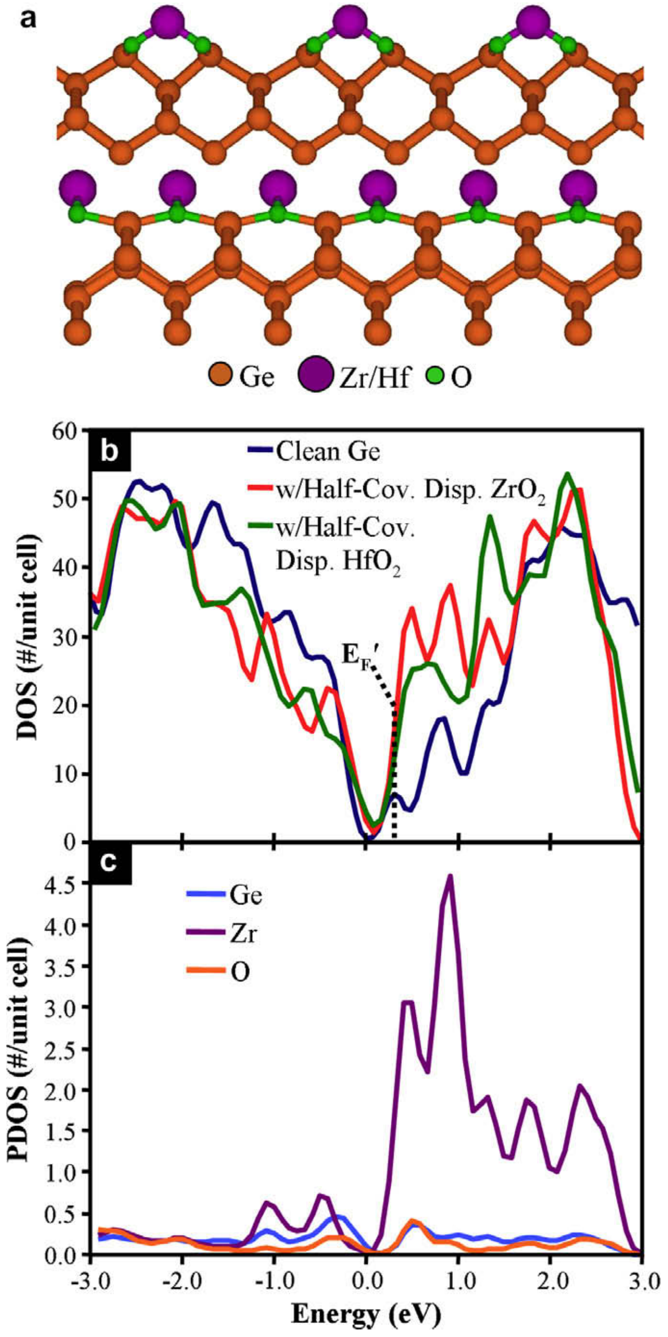

Fig. 5. (a) Ball-and-stick diagrams of the half-coverage displacement-type M–O–Ge geometry. (b) DFT calculated densities of states for half-coverage displacement-type M–O–Ge ZrO_2 and HfO_2. (c) Projected density of states for ZrO_2 case (note: HfO_2 results nearly identical).

this system (see Fig. 5c) shows that increase in CB density is due entirely to the metal atoms, while the reduction in VB density appears to have occurred at the second layer Ge atoms to which the O atoms are bonded. These results are entirely consistent with large charge withdrawal from both the metal and Ge atoms by the electronegative O atoms. However, the induced near-E_F DOS changes are nowhere near as extreme as those for pure high-coverage O_2 displacement configurations. This is most likely due to the fact that the metal atoms act as good electron donors to the O atoms reducing the charge withdrawal from the Ge atoms (and thus reducing the ionic character of the O–Ge bonds), thereby decreasing the perturbation of the Ge electronic structure.

3.2.2. Half-coverage M–O–Ge adsorption

To simulate a simple non-displacement M–O–Ge interface, ZrO_2 and HfO_2 molecules were adsorbed to the Ge(1 0 0)-4 × 2 surface oxygen-down (see Fig. 6a). In this geometry, the O atoms bind directly to the Ge dangling bonds, the MO_2 molecules bridge the trough between dimer rows, and the M atoms point upward away from the surface. This adsorbate system only utilizes half of the number of available Ge bonding sites (i.e. the Ge–Ge surface dimers are left intact), and is therefore also denoted as half-coverage. This geometry yielded enthalpies of adsorption for the MO_2/Ge(1 0 0) system of −2.97 eV/ZrO_2 and −3.67 eV/HfO_2, within only 0.2 eV of the half-coverage O–M–Ge geometries.

The half-coverage M–O–Ge geometry is found to display distinct densities of states for the ZrO_2 and HfO_2 systems. Seen in Fig. 6b, the ZrO_2/Ge(1 0 0) system possesses a slightly shifted near-E_F DOS minimum compared to the

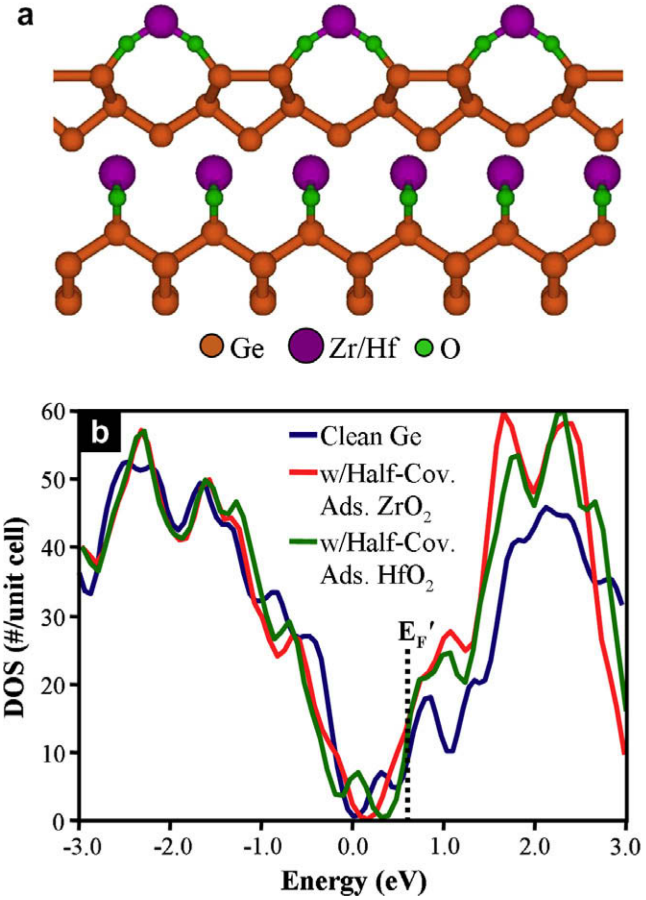

Fig. 6. (a) Ball-and-stick diagrams of the half-coverage adsorbate-type M–O–Ge geometry. (b) DFT calculated densities of states for half-coverage adsorbate-type M–O–Ge ZrO_2 and HfO_2.

clean Ge(100) surface. The HfO_2/Ge(100) system also possesses a near-E_F DOS minimum, shifted 0.3 eV up from the clean Ge(100) DOS minimum, but there exists a new peak centered at the clean Ge(100) Fermi level position. The rest of the two densities of states are nearly identical.

Examination of the ZrO_2/Ge(100) system PDOS, presented in Fig. 7a, clearly shows that the vast majority of the surface electronic state density belongs to the metal (Zr) atoms. The same holds true for the HfO_2/Ge(100) case (see Fig. 7b). The Ge and O band edge states for the two systems are nearly identical and comparatively small. The 0 eV position in the Zr PDOS shows a state density minimum, but the same location for the Hf case displays a distinct, unexpected peak. This peak may correspond to the small shoulder in the CB PDOS for the Zr system, denoted in Fig. 7a by the arrow. HfO_2(g) has a smaller HOMO–LUMO splitting (about half) than ZrO_2(g), consistent with these adsorbates have distinct electronic structures. However, it is also possible that the small 0 eV state for HfO_2/Ge in seen Fig. 6b is due to the previously-discussed errors in the density functional theory.

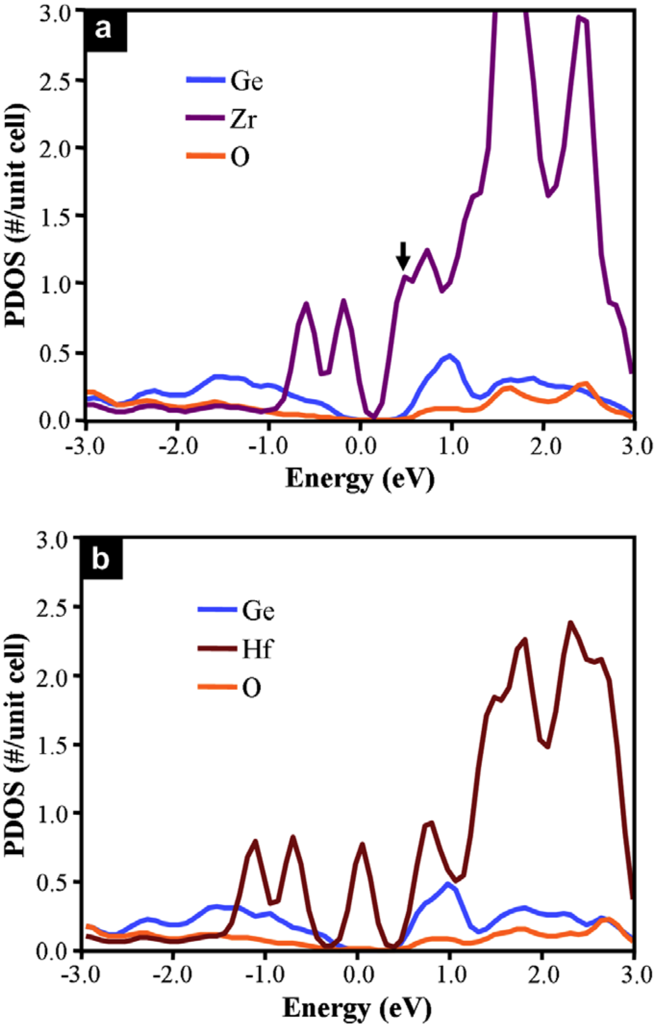

Fig. 7. DFT calculated projected densities of states of the half-coverage adsorbate-type M–O–Ge geometry for (a) ZrO_2 and (b) HfO_2. The arrow in (a) points to the shoulder potentially belong to an electronic state equivalent to that found for HfO_2 at 0.0 eV.

3.2.3. Half-coverage H–M–O–Ge adsorption

Similar to the upward pointing oxygen atoms in the O–M–Ge configuration, the metal atoms in the M–O–Ge configuration are expected to possess partially-filled dangling bonds. In bulk MO_2, each metal atom makes four bonds to neighboring oxygen atoms. Therefore, in order to explore the effect of the dangling bonds on the electronic structure of the interface, the metal atoms were passivated with two H atoms each (see Fig. 8a). We note this bond termination should act as a simulation of further oxide growth, but with the caveat that H atoms are not as good of electron acceptors as O atoms.

Fig. 8b presents the calculated total densities of states for the two H-passivated M–O–Ge MO_2/Ge(100) adsorbate geometries. We see that the H passivation has reduced some of the empty-state (CB) state density, as well as opened true band gaps for both systems, though these gaps do not align with the clean Ge(100)-4 × 2 Fermi level. We know that these are true band gaps because the DOS goes

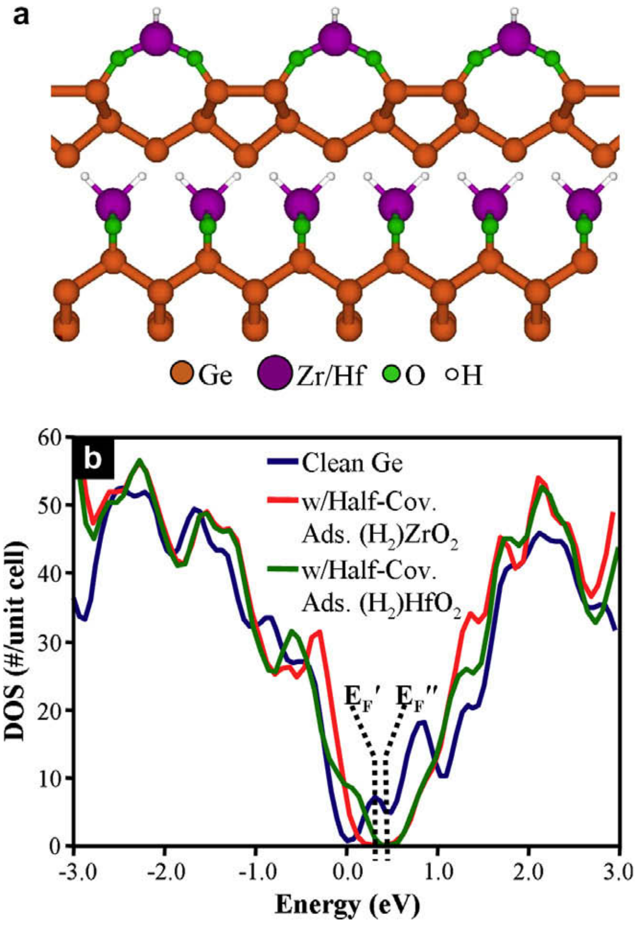

Fig. 8. (a) Ball-and-stick diagrams of the half-coverage adsorbate-type H–M–O–Ge geometry. (b) DFT calculated densities of states for half-coverage adsorbate-type H–M–O–Ge ZrO_2 and HfO_2. Note the opening of the semiconducting band gap and minima shifts for both species.

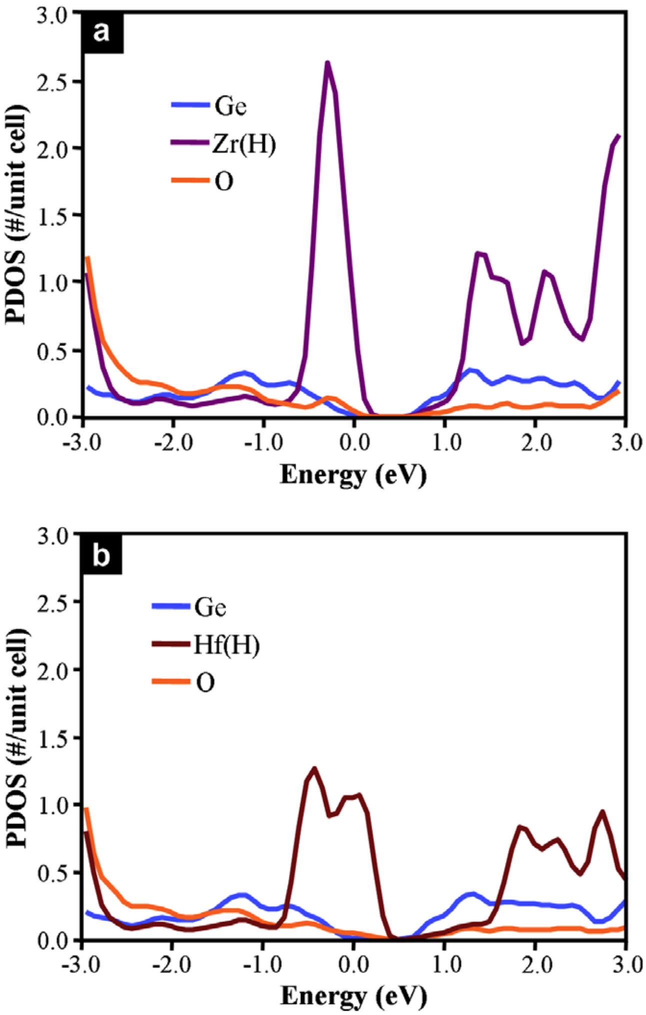

Fig. 9. DFT calculated projected densities of states of the half-coverage adsorbate-type H–M–O–Ge geometry for (a) ZrO_2 and (b) HfO_2.

to zero at the minimum, the calculated Fermi level lies in the middle of the minimum, and the Kohn–Sham orbitals in that energy range are empty. It is interesting that a band gap should form for these systems given the lack of true gap for the clean Ge case, but we note that the formation of this gap is consistent with the strong covalent binding of the metal oxide, removing the metallic character of the flat Ge dimers. However, even with the opening of the band gaps, we see that the ZrO_2 and HfO_2 systems are still not equal; the HfO_2 still retains a distinct state at the 0 eV position, as it did in the non-H-passivated case, while the ZrO_2 system does not.

Analysis of the Zr and Hf PDOS plots for the H–M–O–Ge systems, shown in Fig. 9, reveals that the H passivation greatly reduced the CB density for the metal atoms, which resulted in the opening of the semiconducting band gaps. The VB doublet peaks seen in the non-passivated PDOS (Fig. 7) were also coalesced into single peaks due to the H passivation. However, the anomalous Hf peak at the 0 eV position remains (see Fig. 9b), though it has somewhat merged with the new VB peak, causing the narrowing of the HfO_2/Ge(100) system band gap and the VB edge shoulder seen in the total DOS.

We also note that, especially for the H-passivated case, we see a similar shift in DOS minima for the M–O–Ge adsorbate systems as was observed for the O–M–Ge case. These shifts, too, may be consistent with surface band bending.

4. Conclusions

We have performed a survey of various transition metal dioxide (ZrO_2 and HfO_2) ordered molecular adsorbate bonding configurations on the Ge(100) surface in order to both provide some potential insight into the high-*k*/Ge interface, as well as computational precursors to further calculations using thick amorphous oxide layers. The calculated enthalpies of adsorption show that bonding geometries with metal–Ge bonds (O–M–Ge) are just as thermodynamically favorable as ones with oxygen–Ge bonds (M–O–Ge), therefore a method of chemical processing may be needed to control the bonding at the interface. The calculated electronic structure results indicate that adsorbate surface bonding geometries of the form O–M–Ge tend to create a metallic (large near-E_F DOS) interface due to the metallic nature of the metal–Ge bonds, which worsens with increasing MO_2 coverage. Adsorbate surface bonding geometries of the M–O–Ge sort appear to produce much more favorable electronic structures (at least for the case of ZrO_2), including the opening of semiconducting band gaps for the H-passivated systems. Shifts in the DOS minima for both O–M–Ge and M–O–Ge adsorbate geometries are consistent with surface band bending induced by the adsorbate films, where such band bending extends much further into the Ge substrate than can be modeled by the eight layer intrinsic Ge slabs used for this computational work.

Acknowledgements

The authors would like to acknowledge the SRC, MARCO, and Intel/UCDISCOVERY for funding this work.

References

[1] R.H. Kingston, J. Appl. Phys. 27 (2) (1956) 101.
[2] P.W. Loscutoff, S.F. Bent, Annu. Rev. Phys. Chem. 57 (1) (2006) 467.
[3] K. Prabhakaran, F. Maeda, Y. Watanabe, T. Ogino, Appl. Phys. Lett. 76 (16) (2000) 2244.
[4] V. Craciun, I.W. Boyd, B. Hutton, D. Williams, Appl. Phys. Lett. 75 (9) (1999) 1261.
[5] O.J. Gregory, E.E. Crisman, L. Pruitt, D.J. Hymes, J.J. Rosenberg, Mater. Res. Soc. Symp. Proc. 76 (1987) 307.
[6] Y. Wang, Y.Z. Hu, E.A. Irene, J. Vac. Sci. Technol., A 12 (4) (1994) 1309.
[7] D.B. Alford, L.G. Meiners, J. Electrochem. Soc. 134 (4) (1987) 979.
[8] S. Huiling, H. Okorn-Schmidt, K.K. Chan, M. Copel, J.A. Ott, P.M. Kozlowski, S.E. Steen, S.A. Cordes, H.S.P. Wong, E.C. Jones, W.E. Haensch, IEEE IEDM (2002) 441.

[9] C.M. Ransom, T.N. Jackson, J.F. DeGelormo, IEEE Trans. Electron Dev. 38 (12) (1991) 2695.

[10] R.S. Johnson, H. Niimi, G. Lucovsky, J. Vac. Sci. Technol., A 18 (4) (2000) 1230.

[11] M.L. Lee, C.W. Leitz, Z. Cheng, A.J. Pitera, T. Langdo, M.T. Currie, G. Taraschi, E.A. Fitzgerald, D.A. Antoniadis, Appl. Phys. Lett. 79 (20) (2001) 3344.

[12] R.A. McKee, F.J. Walker, M.F. Chisholm, Science 293 (5529) (2001) 468.

[13] M. Meuris, A. Delabie, S. Van Elshocht, S. Kubicek, P. Verheyen, B. De Jaeger, J. Van Steenbergen, G. Winderickx, E. Van Moorhem, R.L. Puurunen, B. Brijs, M. Caymax, T. Conard, O. Richard, W. Vandervorst, C. Zhao, S. De Gendt, T. Schram, T. Chiarella, B. Onsia, I. Teerlinck, M. Houssa, P.W. Mertens, G. Raskin, P. Mijlemans, S. Biesemans, M.M. Heyns, Mater. Sci. Semicond. Proc. 8 (1–3) (2005) 203.

[14] K.C. Saraswat, C.O. Chui, T. Krishnamohan, A. Nayfeh, P. McIntyre, Microelectron. Eng. 80 (2005) 15.

[15] Y. Kamata, Y. Kamimuta, T. Ino, A. Nishiyama, Jpn. J. Appl. Phys. 44 (4B) (2005) 2323.

[16] C. Chi On, H. Kim, D. Chi, P.C. McIntyre, K.C. Saraswat, IEEE Trans. Electron Dev. 53 (7) (2006) 1509.

[17] G. Kresse, Thesis, Technische Universität Wien, 1993.

[18] G. Kresse, J. Furthmüller, Phys. Rev. B 54 (16) (1996) 11169.

[19] G. Kresse, J. Furthmüller, Comput. Mater. Sci. 6 (1) (1996) 15.

[20] G. Kresse, J. Hafner, Phys. Rev. B 47 (1) (1993) 558.

[21] P.E. Blöchl, Phys. Rev. B 50 (24) (1994) 17953.

[22] G. Kresse, D. Joubert, Phys. Rev. B 59 (3) (1999) 1758.

[23] J. Paier, R. Hirschl, M. Marsman, G. Kresse, J. Chem. Phys. 122 (23) (2005) 234102.

[24] D.L. Winn, M.J. Hale, T.J. Grassman, A.C. Kummel, R. Droopad, M. Passlack, J. Chem. Phys. 126 (8) (2007) 084703.

[25] J.P. Perdew, M. Levy, Phys. Rev. Lett. 51 (20) (1983) 1884.

[26] L.J. Sham, M. Schlüter, Phys. Rev. Lett. 51 (20) (1983) 1888.

[27] O. Gurlu, H.J.W. Zandvliet, B. Poelsema, Phys. Rev. Lett. 93 (6) (2004) 066101.